

# Characterization of a Space Pulsating Heat Pipe on board REXUS 22 Sounding Rocket

P Nannipieri<sup>1</sup>, M Anichini<sup>1</sup>, L Barsocchi<sup>1</sup>, G Becatti<sup>1</sup>, L Buoni<sup>1</sup>, F Celi<sup>1</sup>, A Catarsi<sup>1</sup>, P Di Giorgio<sup>1</sup>, P Fattibene<sup>1</sup>, E Ferrato<sup>1</sup>, P Guardati<sup>1</sup>, E Mancini<sup>1</sup>, G Meoni<sup>1</sup>, F Nesti<sup>1</sup>, S Piacquadio<sup>1</sup>, E Pratelli<sup>1</sup>, L Quadrelli<sup>1</sup>, A S Viglione<sup>1</sup>, F Zanaboni<sup>1</sup>, M Mameli<sup>1</sup>, F Baronti<sup>1</sup>, L Fanucci<sup>1</sup>, S Marcuccio<sup>1</sup>, C Bartoli<sup>1</sup>, P Di Marco<sup>1</sup>, S Filippeschi<sup>1</sup>, M La Foresta<sup>2</sup>, L Caporale<sup>2</sup>, N Bianco<sup>3</sup> and M Marengo<sup>4</sup>,

<sup>1</sup> University of Pisa, Largo Lucio Lazzarino 2, 56122 Pisa, Italy.

<sup>2</sup> AAVID Thermalloy, Via del Fonditore, 4, 40138, Bologna, Italy.

<sup>3</sup> University of Naples Federico II, Corso Umberto I, 40, 80138, Naples, Italy.

<sup>4</sup> University of Brighton, Lewes Rd, Brighton BN2 4AT, United Kingdom.

[mauro.mameli@ing.unipi.it](mailto:mauro.mameli@ing.unipi.it)

**Abstract.** Micro-gravity environments might extend the concept of capillary behavior structure to large diameter tubes. A Loop Thermosyphon, in its traditional use, is a two-phase thermal device which usually consists of a large tube, closed end to end in a loop, evacuated and partially filled with a working fluid and intrinsically gravity assisted. With the concept stated here, it may become a capillary tube in space condition and turn its thermo-fluidic behavior into a Pulsating Heat Pipe (PHP), or better, a Space Pulsating Heat Pipe (SPHP). The present work presents the results of the experimental campaign of a SPHP effectuated both on ground and in microgravity conditions. A SPHP has been designed and implemented on board of a sounding rocket launched in the 22<sup>nd</sup> ESA REXUS Sounding Rocket Campaign. This type of sounding rocket launch guarantees approximately 120s of microgravity environment. The ground tests prior to the launch demonstrated that the device effectively work as a gravity assisted loop thermosyphon, while the experimental data from the microgravity period during the sounding rocket launch reveal a change in the thermal hydraulic behavior similar to the PHP. The micro-g environment provided by the rocket was not sufficient to reach a pseudo steady state regime, therefore, further investigation on a longer term weightless condition is mandatory.

## 1. Introduction

Technological innovation has led to a trend for electronic components miniaturization, eventually causing a considerable increase of heat power per unit surface area to be dissipated in order to ensure safe temperature ranges during operations. This issue is especially critical for space applications. To date, sintered wick Heat Pipes (HP) and Loop Heat Pipes (LHP) are generally preferred because of their lightweight, reliability and, most of all, their ability to operate without the assistance of any acceleration field [1]. This ability is obtained by means of a capillary structure which is also the most complex and expensive element inside the system. In a cost reduction perspective, Akachi [2,3], introduced the concept of Pulsating Heat Pipe (PHP), which is basically a wickless two phase loop, consisting of a capillary diameter tube bended in several turns so that the fluid resides inside the tube as an alternation of liquid slugs and vapor bubbles: when the vapor formed in the heated zone expands, it pushes the adjacent fluid to the condenser zone, where the heat is released and the vapor condenses. On ground conditions, a small diameter is required in order to ensure capillarity to be predominant with respect to

buoyancy forces (i.e., a Bond Number less than a critical value is required) and obtain a confined liquid slug-vapor plugs flow regime. The literature generally estimates the static critical tube diameter (i.e., the maximum PHP tube diameter allowed for efficient ground operations) from the Kews and Cornwell [4] criterion:

$$Bo = \frac{g(\rho_l - \rho_v)d^2}{\sigma} < 4 \quad (1)$$

where  $\sigma$  is the liquid surface tension,  $g$  is the gravitational acceleration and  $\rho_l$  and  $\rho_v$  are respectively the liquid and vapor density. From the previous equation, it seems evident that the microgravity condition may allow for a bigger critical diameter and, consequently, for an higher thermal flux dissipation [5]. On the other hand, the previous criterion may not be the most suitable in microgravity conditions since it does not consider the inertial and viscous effects: it was proposed in fact [6] a more comprehensive criterion based on the Garimella number:

$$Ga = \sqrt{Bo}Re < 160 \quad (2)$$

where  $Re = \rho_l U_l d / \mu_l$  is the Reynolds number related to the liquid phase. Figure 1 shows the resulting static and dynamic critical diameters ( $d_{Bo}$  and  $d_{Ga}$ , calculated respectively by means of equation 1 and 2) for  $C_6F_{14}$  at  $20^\circ C$  and for an average liquid phase velocity equal to 0.1 m/s. Indeed, even by considering the most conservative criterion, it should be theoretically possible to develop a two-phase loop working as a Pulsating Heat Pipe (slug/plug flow pattern) even if the tube diameter is bigger than the critical value calculated in ground conditions (Space PHP).

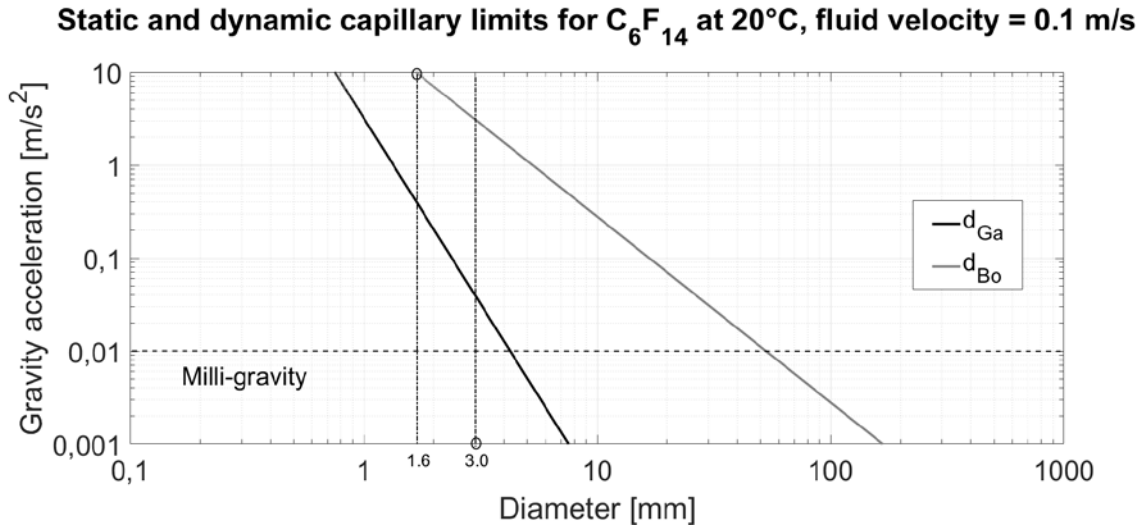


**Figure 1:** Static and dynamic capillary limits for  $C_6F_{14}$  at  $20^\circ C$ , fluid velocity = 0.1 m/s.

Several experiments in microgravity condition (i.e. by means of parabolic flight or sounding rockets) have been carried out on capillary PHPs [5, 7-13] and most of them clearly revealed a self-sustained two-phase flow motion in microgravity. Few experiments have instead been performed with a tube diameter larger than the critical one on ground. In detail, the Space PHP concept feasibility has been successfully tested by Mangini *et al.* [14,15], who tested a PHP with an inner diameter of 3mm charged with  $C_6F_{14}$  (not capillary on ground, see Figure 1), both on ground and in milli-gravity condition during ESA 61th and 63th Parabolic flight campaign. They noticed that a sudden transition of the flow pattern from stratified to slug flow takes place as the microgravity occurs, showing that the device may work as a PHP in space conditions. Anyway, the reduced gravity ambient experienced during the parabolic flight (about 20 s) was too short to reach a steady state conditions, which would be useful to characterize the thermal performances of the device. Considering the above, the first experiment on the Space PHP

onboard a sounding rocket was performed (REXUS 18) in order to obtain data on a longer microgravity duration (120s), but it failed due to a problem in the rocket de-spinning system [16]. An updated experiment on the Space PHP has been designed, built and tested during the REXUS 22 campaign [17,18]. The present work is thus devoted at describing the experimental setup which flew on board REXUS 22 sounding rocket and its outcomes both on ground and microgravity conditions.

## 2. Experimental setup and procedure

### 2.1. Overview

The designed experimental setup mainly consists of:

- A PHP test cell;
- A heat sink, realized by means of a Phase Change Material (PCM) doped with a metallic foam;
- A heat source, which is also used prior to the launch in order to maintain the PCM at temperature ranges close to the PCM melting point (preheating);
- A power supply, realized by means of a battery pack and the related electronics (PDU, Power Distribution Unit);
- An on board data handling and acquisition system;
- A real-time software controlling all of the processes via a Main Control Unit (MCU);
- A system interface with the REXUS rocket.

### 2.2. Test Cell

The PHP test cell is a single loop aluminum tube (6060 alloy) folded in a staggered configuration with fourteen U-turns at the evaporator and thirteen U-turns at the condenser, Figure 2. The device is evacuated and then partially filled with the working fluid (n-perfluorohexane,  $C_6F_{14}$ ) at a volumetric ratio of  $0.5 \pm 0.025$  (corresponding to 8.3 ml), via a T-junction.

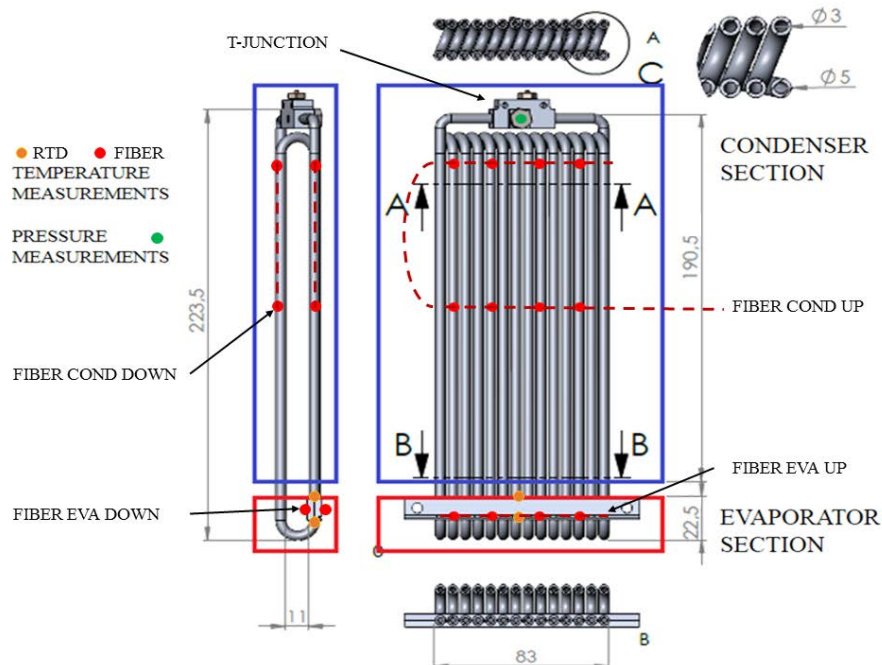


**Figure 2:** PHP Test Cell Layout, geometry and measurements location

The PHP condenser section is embedded into the heat sink, consisting of a PCM (octadecane paraffin wax) doped with a metallic foam (ERG<sup>®</sup>, aluminum, 40 Pores Per Inch, 12% relative density). It is well known that, among the PCMs, paraffin waxes show many advantages, such a high latent heat, a low vapor pressure, stable and non-toxic chemical properties. However, their thermal conductivity is very low.

The metallic foam is thus employed to effectively increase the overall thermal conductivity of the heat sink [21]. In order to avoid any leakage of PCM, the condenser section of the PHP and the heat sink are contained inside an airtight box. Two ceramic heaters, powered by the power supply, are mounted on the heating plates brazed just above the U-turns in the evaporator zone, Figure 3.

### 2.3. Power Supply

An electric power input up to 200 W is provided by a battery pack (8s1p SAFT Li-Ion cells, 28 V, 54.4 Ah), while a custom electronic PCB, provided with a PWM at 225 Hz, is employed to supply a wide range of power levels to the ceramic heaters. The same board has the role of exploiting power measurements, with an estimated accuracy of about 5%. The maximum achievable radial wall-to-fluid local heat flux at the evaporator section of the PHP has been estimated to be equal to 12.6 W/cm<sup>2</sup>.

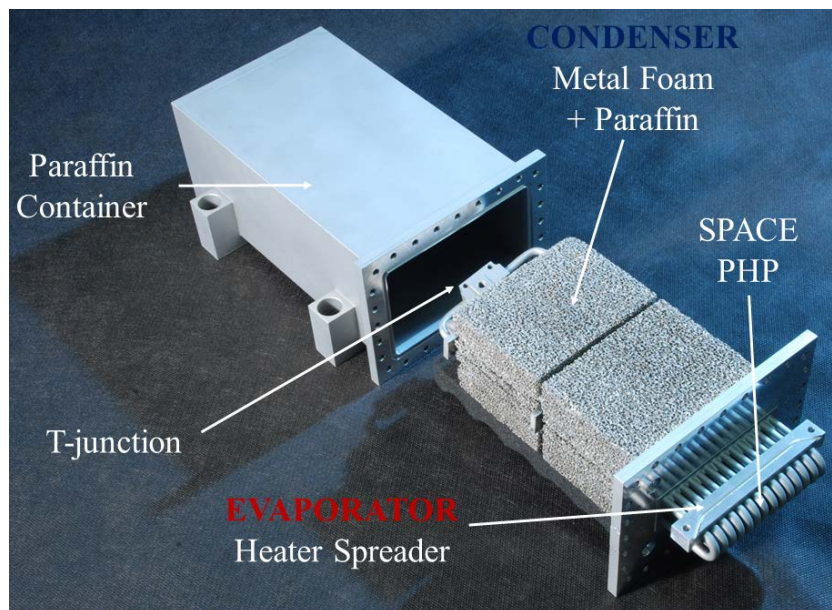


**Figure 3:** PHP test cell actual shape and main components.

### 2.4. Acquisition and Data Handling

Pressure and temperature of the PHP working fluid are acquired in several points during the flight, Figure 2. In particular, a pressure transducer (Kulite<sup>®</sup>, XCQ-093-1.7 bar A, max error 0.5% FSO), is located in the T-junction at the condenser end of the PHP, while a Fiber Bragg Grating (FBG) temperature measurement system (SmartScan<sup>®</sup> series realized by Smart Fibres<sup>®</sup> and Infibra Tec. <sup>®</sup>) acquires temperatures in 24 points by means of optical sensors, with an accuracy of  $\pm 0.1$  K. This system has many technological advantages such as the intrinsic immunity to electromagnetic interference, compactness, easy integrability and accuracy. Up to the authors' knowledge, this is the first time that this system is used to test a PHP and the first time that it is used on board a space vehicle as temperature sensor [19]. The FBG interrogator can handle a maximum scanning frequency of 2.5KHz for all sensors simultaneously. Two PT-100 ( $\pm 0.06\Omega$  @ 0°C) are placed in the evaporator section for FBG calibration and redundancy. A data handling system records the output of the optical sensors (at 10Hz), pressure transducer (at 100Hz) and g-sensor (at 10Hz). Moreover, gravity variations during the flight are detected by means of a three-axis g-sensor (Dimension Engineering<sup>®</sup>, DE-ACCM3d, sense range:  $\pm 3g$ , sensitivity 333mV/g). This sensor is employed in order to detect the switching from hyper gravity to

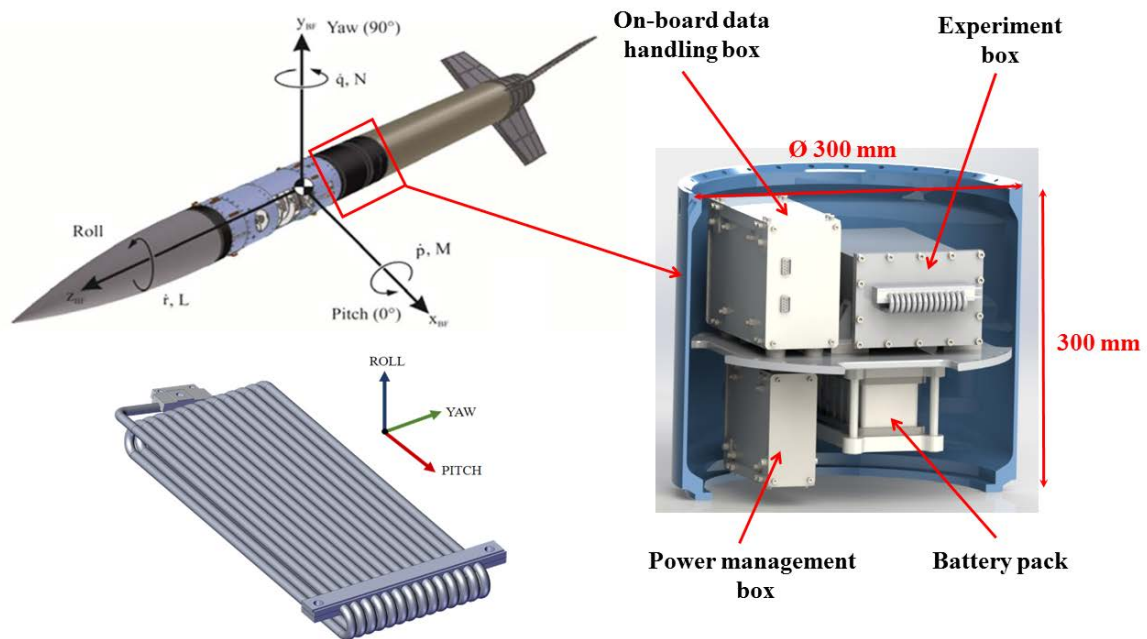


**Figure 4:** Rocket scheme and acceleration references (left) and U-PHOS module scheme (right)

milligravity condition at the engine burn-out and the accelerations on the three axes when the de-spin has taken place, Figure 4.

### 2.5. Experiment Timeline

A custom-made ground software developed with LabVIEW® controls the experiment during the pre-launch phase and it receives, displays and stores all the data acquired during the flight. In detail, the experiment timeline is structured as follows:

- From  $t = -900 \text{ s}$  to the lift-off ( $t = 0 \text{ s}$ ): the preheating system is activated. A low percentage of the nominal power (80 W) is provided by the batteries to the heater to keep the PCM temperature as close as possible to the melting point ( $28^\circ\text{C}$ ) and to keep the other experiment components within their temperature operative range. This percentage is adjustable at need via uplink while the rocket is on the launch pad;
- From  $t = 0 \text{ s}$  to  $t \sim 65 \text{ s}$ : at lift-off, the PHP is heated at full power (200 W). Data acquisition, data storage and downlink are switched on. After the engine burnout ( $t=26 \text{ s}$ ), the experiment is in milli-g conditions, but the rocket is still spinning. At  $t\sim 65\text{s}$  the de-spin system is activated.
- From  $t \sim +65 \text{ s}$  to  $t = +190 \text{ s}$ : The whole experiment is in milli-gravity condition. Due to the low thermal inertia of the heating system and of the device, pseudo-steady state condition is expected;
- $t = +300 \text{ s}$ : the experiment is switched off and all the data are once again sent to ground for redundancy.

## 3. Experimental Results

The results of the ground test and flight experiment are presented in this section. The ground test was effectuated in vertical bottom heated mode, which corresponds to the best operative ground condition for the device, and is a good benchmark to compare with the performance in flight of the SPHP.

### 3.1. Ground tests

Due to the gravity environment and the large tube diameter, buoyancy forces are predominant with respect to surface tension forces. Therefore, during vertical operation on ground the liquid phase and vapor phase occupy respectively the lower part (evaporation section) and the higher part (condenser section) of the PHP. In the evaporation section the liquid phase boils continuously and generates vapor.



The vapor rises toward the condenser dragging liquid batches in the so-called “bubble lift” mode [20] and, due to the loop configuration, a very efficient flow circulation is obtained.

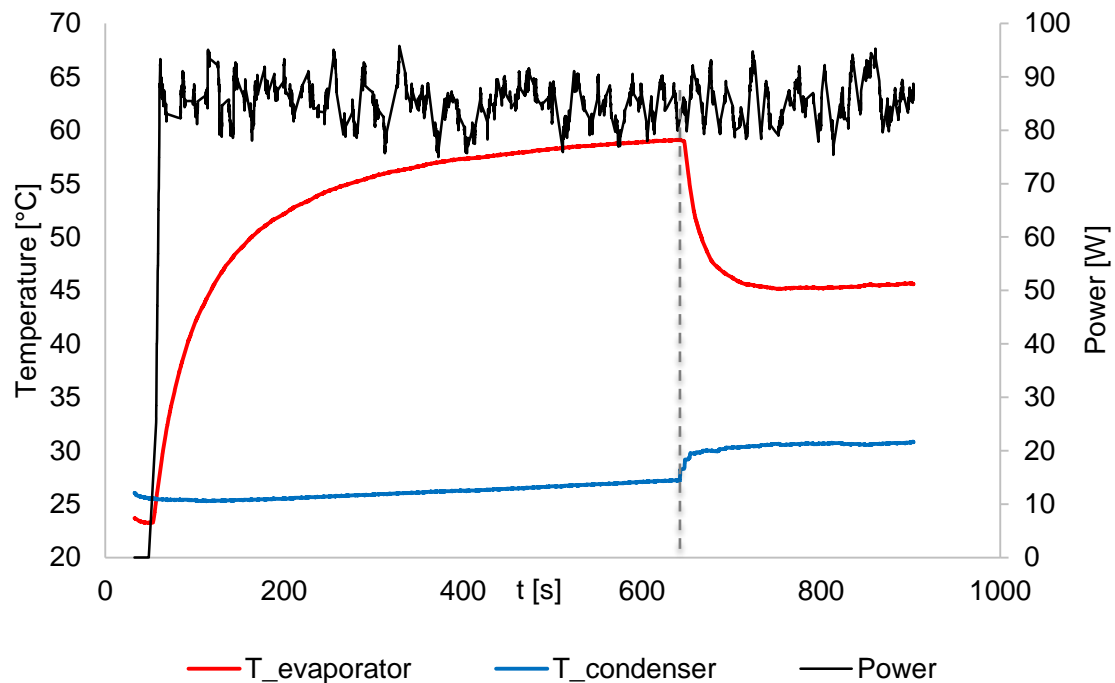


**Figure 5:** Start-up in ground conditions, bottom heated mode, 90W

The results of the preliminary test performed on the device in bottom heated mode at 90W are shown in Figure 5. In particular, the red line represents the average temperature in the evaporator section, the blue line is the average temperature in the condenser zone, and the black line is the actual power provided to the evaporator zone. Regarding the start-up time of the device, it is highlighted by the dashed line and it is of the order of 600 s. As can be seen, when the boiling process occurs, the gravity assisted two phase flow motion enhances the device thermal performance, halving the overall thermal resistance from 0.33 K/W to 0.16 K/W.

From this first ground experiment, it is clear that the device may work fairly good in a gravity assisted configuration, opening to the possibility of a hybrid device capable of working on ground as a thermosyphon and switching to a SPHP in a micro-g environment.

### 3.2. Flight test

The first micro-g test was developed on a similar device mounted in the REXUS 18 sounding rocket [16]. However, due to a malfunction in the de-spin system, during the whole flight the rocket experienced a centrifugal acceleration, which affected the fluid distribution and compromised the experiment outcome. In later experiments, a comparable SPHP was tested on board of parabolic flights [14,15]. The outcome data shows the expected transition to the slug and plug flow pattern, observable from the sudden transition in the temperatures and pressure. The same trend is visible from the results obtained from the REXUS 22 sounding rocket flight. In detail, Figures 6 to 9 shows the temporal evolution of the main operative parameters: Figure 6b shows the temperature in the evaporator zone; Figures 7b and 8b show the temperature in the condenser zone on the upper and lower tube rank; Figure 9b shows the local fluid pressure in the condenser zone. In every figure, the secondary y-axis corresponds to the heating power level, represented with the dark line.

### 3.2.1. Phase 1: until Lift Off.

In the first phase before the Lift Off (LO in the figures), the rocket, standing in vertical position, experiences only the Roll acceleration component, equal to 1g. The device is now preheated at 80W to keep the PCM temperature as close as possible to the melting point (28°C), and the condenser temperatures are successfully maintained very close to that point as shown in Figures 7 and 8. In this configuration the device is horizontally oriented and the internal diameter is bigger than the capillary limit on ground. Thus, the two-phase flow stratifies within the tube, with the liquid in the lower tube rank. Moreover, it is known in the literature that a two-phase thermosyphon does not work if the heated zone is above the condenser. Thus, the heat is transferred only by means of conduction. During the preheating operation, the evaporator temperature is indeed rising homogeneously, up to 50°C (Figure 5) and the fluid pressure signal (Figure 8) is not showing any variation rather than its white noise ( $\pm 500$  Pa).

### 3.2.2. Phase 2: from Lift Off to De-Spin

From the Lift Off the device is supplied with the regime heating power input (200 W), consequently both the evaporator and condenser temperatures rise. Between the Lift Off and the De-Spin (DS in the figures) the acceleration level experienced by the rocket reaches nearly 20 g of vertical acceleration due to the thrusting phase of the motor and up to 6 g of centrifugal acceleration, due to the rocket spinning. The former is perpendicular to the flow path direction and increments the stratified behavior of the fluid. The latter tends to push the liquid phase on the periphery of the device. The effect of this acceleration field on the thermo-fluidic behavior is unpredictable but, on the overall, it is certainly assisting the fluid motion, as seen by comparing the temperature trends in the subsequent microgravity period.

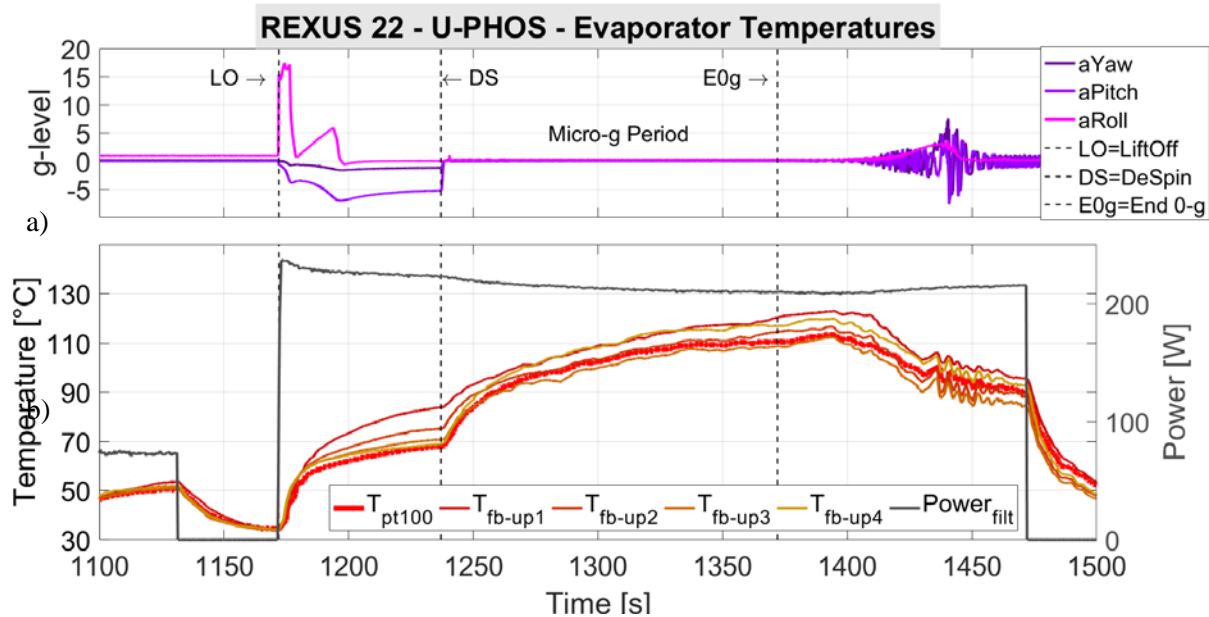


**Figure 6:** a) Accelerations during the different phases; b) Evaporator temperature trends (left y-axis) and Heating power (right y-axis).

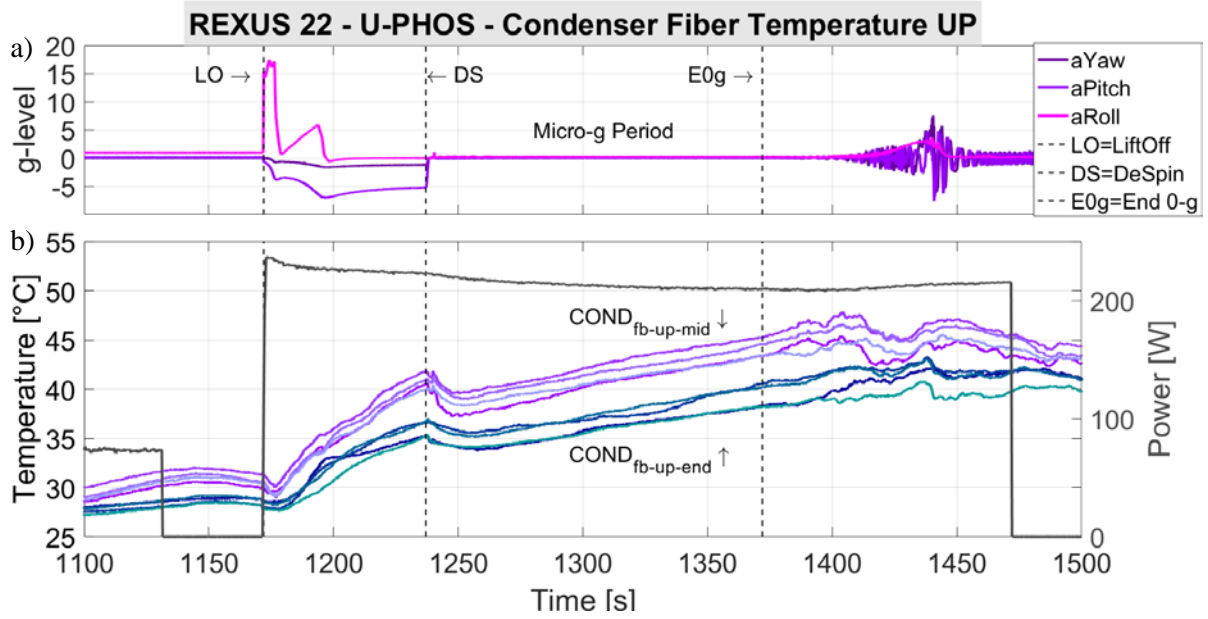


**Figure 7:** a) Accelerations during the different phases; b) Condenser temperature trends on the upper tube rank (left y-axis) and Heating power (right y-axis).

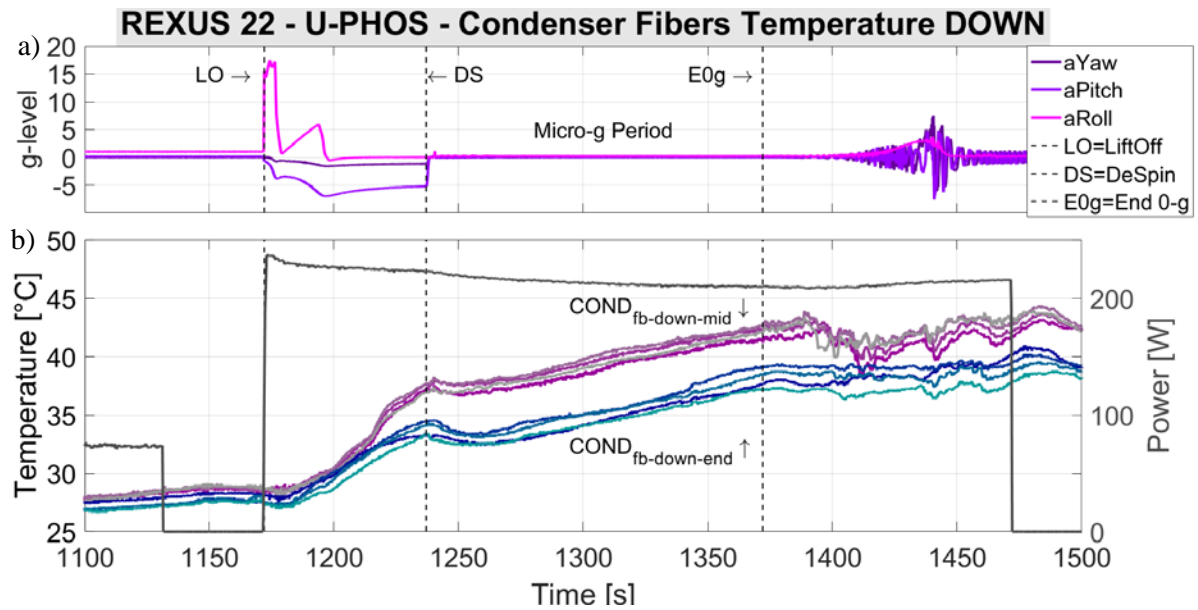


**Figure 8:** a) Accelerations during the different phases; b) Condenser temperature trends on the lower tube rank (left y-axis) and Heating power (right y-axis).



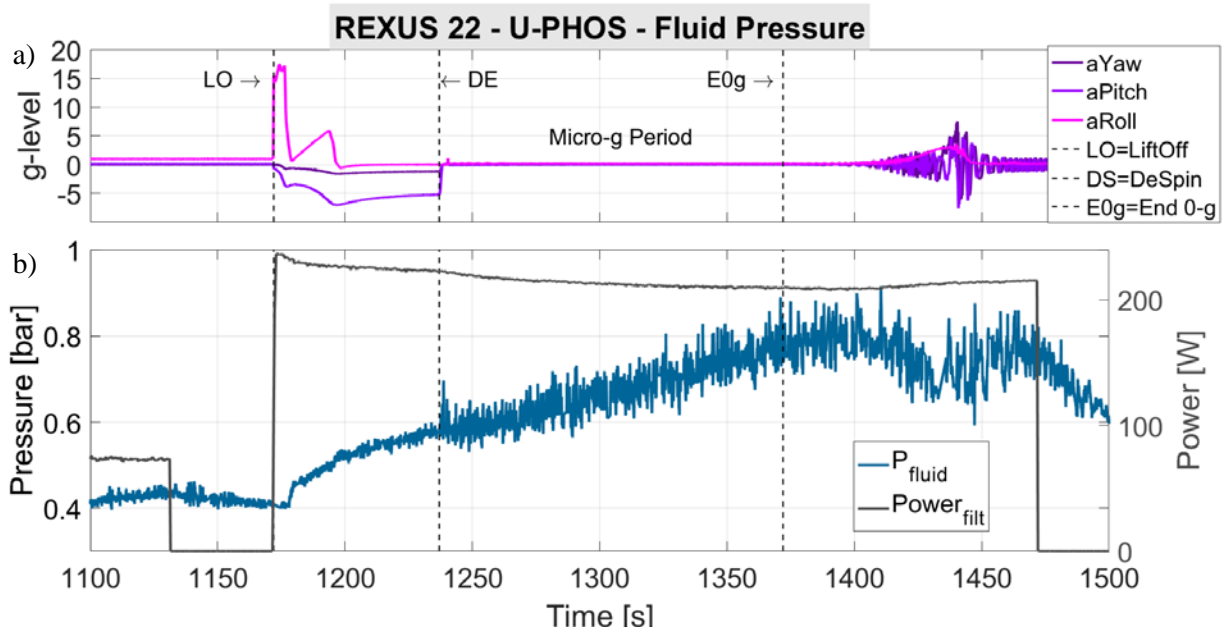


**Figure 9:** a) Accelerations during the different phases; b) Local fluid pressure trend (left y-axis) and Heating power (right y-axis).

### 3.2.3. Phase 3: from De-Spin to Reentry

The rocket De-Spin activation terminates the centrifugal accelerations on the rocket: the three acceleration components decrease and the milligravity condition is reached. As seen from Figures 6, 7 and 8, immediately after the De-Spin the overall heat transfer performance suddenly decreases with respect to the previous period. In fact, the evaporator temperature exhibits a sudden increase, while the condenser temperature decreases. Therefore, it is reasonable to assess that the acceleration field during the launch phase has positive effect on the fluid motion and consequently on the device heat transfer rate, while the overall device performance seems to degrade during the milligravity period. However, the experimental data show interesting trends in the milli-g environment both in term of temperature and pressure of the fluid. In fact, temperatures in both the evaporator and condenser, as well as the fluid pressure exhibit an oscillating component for the whole zero gravity duration. These trends confirm that that a multi-turn two phase loop is able to work as a Space PHP in milligravity conditions. Unfortunately, it was not possible to reach a pseudo-steady state (probably because of the thermal inertia of the heat sink), stressing the fact that, coherently with the results obtained from the ground test, a longer term reduced gravity period is needed in order to infer about the actual heat transfer performance of the device.

### 3.2.4. Phase 4: from Reentry to Landing

The milli-gravity condition ends (E0g in the figures) at the start of the reentry phase. In this period, the rocket experiences a complex acceleration field that, once again unpredictably, assists the fluid motion, decreasing the evaporator temperatures. The Fluid pressure signal shown in figure 9 is one of the most interesting since it clearly reveals a change in the trend immediately after the occurring of milligravity. It is possible to compare the actual results of the rocket launch (Figure 10a) with the one obtained in micro-g conditions during the 63<sup>rd</sup> Parabolic Flight Campaign (PFC) by Mangini *et al.* [14] (Figure 10b). The device tested during the PFC is very similar to the one employed here, with five U-turns at the evaporator, same tube inner diameter (3mm), very similar working fluids (FC-72 and pure perfluorohexane), same wall to fluid heat flux (12.5 W/cm<sup>2</sup>). This comparison shows a comparable trend of the pressure absolute mean level and amplitude.

In particular, during the parabolic flight, the pressure trend recorded displays a slightly higher amplitude and it is characterized by some stop-over periods; interestingly the sounding rocket experiment fluid pressure exhibits a slightly lower amplitude without stop-over periods.

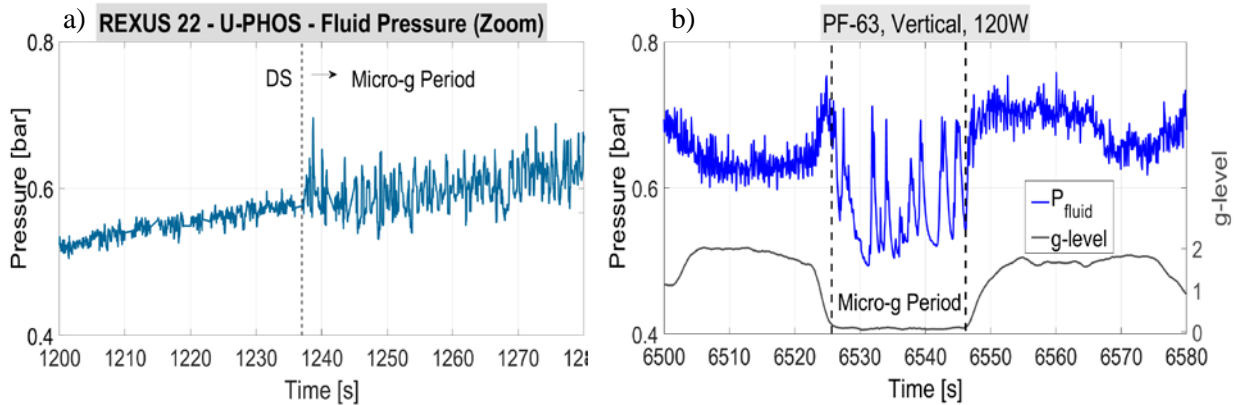


**Figure 10:** Local fluid pressure trend a) REXUS 22. Actual results zoomed on the De-Spin event. b) 63rd Parabolic flight campaign (Mangini et al. 2015).

#### 4. Conclusions

In this paper, the Space PHP concept has been presented together with the main features of the experimental setup which flew on board REXUS 22 sounding rocket. The main goal of the experiment has been to characterize the thermos-hydraulic response of a Large Diameter Pulsating Heat Pipe in milligravity conditions, thus verifying its heat transfer capabilities for space applications.

Preliminary ground tests confirmed that the device successfully works as a two-phase loop thermosyphon if gravity assisted, with an overall thermal resistance of 0.16 K/W at 90W. Moreover, the test in milli-gravity condition on board REXUS 22 sounding rocket (which flew on March 2017) has been successful. Immediately after the De-Spin, all the temperature signals both in the evaporator and condenser have exhibited an oscillating component for the whole zero gravity duration. The amplitude of the fluid pressure signal is evidently increased under the occurrence of the microgravity period and, differently from similar experiments in the literature, is not characterized by stop-over phenomena. Unfortunately, it was not possible to reach a pseudo-steady state probably because of the thermal inertia of the heat sink, stressing the fact that a longer-term micro gravity period is needed to infer about the actual heat transfer performance. Anyway, from the results obtained it is clear that the perspective of having a hybrid device that works effectively on ground as a thermosyphon and switch to a Space PHP in zero gravity conditions is very promising.

#### Acknowledgements

The present work has been carried out as part of the REXUS BEXUS program, supported by European space agency (ESA), German Aerospace Research Establishment (DLR) and Swedish National Space Board (SNSB). The ESA MAP INWIP project for funding the project, the International Scientific Team on Pulsating Heat Pipes, the school of engineering and all the technical sponsors (<http://www.uphos.ing.unipi.it/it/supporters/>). The authors would like to thank the Alessandro Signorini and INFIBRA Technology for the great help and the PHOS team for the support and encouragement.

#### References

- [1] Gilmore G., 2002. *Spacecraft Thermal Control Handbook*, Fundamental Technologies, The Aerospace Press, El Segundo California.
- [2] Akachi H., 1990. Structure of a heat pipe, *US Patent* 4.921.041
- [3] Akachi H., 1993. Structure of a micro heat pipe, *US Patent* 5.219.020.

- [4] Kew, P.A. and K. Cornwell 1997. "Correlations for the prediction of boiling heat transfer in small-diameter channels". *Applied Thermal Engineering*, Vol. **17**, pp. 705–715.
- [5] Gu, J., Kawaji, M., and Futamata, R., 2004. "Effects of gravity on the performance of Pulsating Heat Pipes", *Journal of Thermophysics and Heat Transfer*, Vol.**18**, pp. 370-378.
- [6] Baldassari C. and Marengo M., 2013. "Flow boiling in microchannels and microgravity", *Prog. Energy Combust. Sci.* Vol. **39** (1), pp. 1-36.
- [7] Gu, J., Kawaji, M., Futamata, R., 2005. "Microgravity performance of micro pulsating heating pipe", *Microgravity Science and Technology*, Vol.**16**, pp. 179-183.
- [8] De Paiva, K. V., Mantelli, M. B., H., Slongo, L. K., Burg, S. J., 2010. "Experimental tests of mini Heat Pipe, Pulsating Heat Pipe and Heat Spreader under microgravity conditions aboard suborbital rockets", *Proc. of the 15th International Heat Pipe Conference*, Clemson, South Carolina, USA.
- [9] De Paiva, K., Mantelli, M.B.H., Florez, J.P.M., Nuernberg, G.G.V., 2013. "Mini Heat Pipe Experiments under Microgravity Conditions. What have we Learned?", *Proc. of the 17th International Heat Pipe Conference*, Kanpur, India, 2013.
- [10] Mameli, M., Araneo, L., Filippeschi, S., Marelli, M., Testa, R., Marengo, M., 2014. "Thermal performance of a closed loop pulsating heat pipe under a variable gravity force", *International Journal of Thermal Science*, Vol. **80**, pp. 11-22.
- [11] Taft, B. S., Laun, F.F., Smith, S., 2015. "Microgravity Performance of a structurally Embedded Oscillating Heat Pipe", *Journal of Thermophysics and Heat Transfer*, Vol. **29**(2).
- [12] Ayel, V., Araneo, L., Scalambra, A., Mameli, M., Romestant, C., Piteau, A., Marengo, M., Filippeschi, S., Bertin, Y., 2015. "Experimental study of a closed loop flat plate pulsating heat pipe under a varying gravity force", *International Journal of Thermal Sciences*, Vol. **96**, pp. 23-34.
- [13] Ayel, V., Araneo, L., Marzorati, P., Romestant, C., Bertin, Y., Marengo, M., 2016. "Visualizations of the flow patterns in a closed loop flat plate PHP with channel diameter above the critical one and tested under microgravity", *Proc. of 18 International Heat Pipe Conference and 12 International Heat Pipe Symposium*, South Korea.
- [14] Mangini, D., Mameli, M., Geourgoulas, A., Araneo, L., Filippeschi, S., Marengo, M., 2015. "A pulsating heat pipe for space applications: Ground and microgravity experiments", *International Journal of Thermal Sciences*, Vol. **95**, pp. 53-63.
- [15] Mangini D., Mameli M., Fioriti D., Araneo L., Filippeschi S., Marengo M., 2017. "Hybrid Pulsating Heat Pipe for Space Applications with Non-Uniform Heating Patterns: Ground and Microgravity Experiments", accepted for publication by the *Applied Thermal Engineering*.
- [16] Creatini F., Guidi G.M., Belfi F., Cicero G., Fioriti D., Di Prizio D., Piacquadio S., Becatti G., Orlandini G., Frigerio A., Fontanesi S., Nannipieri P., Rognini M., Morganti N., Filippeschi S., Di Marco P., Fanucci L., Baronti F., Manzoni M., Mameli M., Marengo M., 2015. "Pulsating Heat Pipe Only for Space: Results of the REXUS 18 Sounding Rocket Campaign", *XXXIII UIT Congress*, L'Aquila, Italy, *Journal of Physics: Conference Series* 655 (2015) 012042.
- [17] Nannipieri P., Anichini M., Barsocchi L, Becatti G., Buoni L., Celi F., Catarsi A., Di Giorgio P., Fattibene P. Ferrato E., Guardati P., Mancini E., Meoni G., Nesti F., Piacquadio S., Pratelli E., Quadrelli L., Viglione A. S., Zanaboni F., Mameli M., Baronti F., Fanucci L., Marcuccio S., Bartoli C., Di Marco P., Bianco N., Marengo M., Filippeschi S., 2016. "U-PHOS Project: Development of a Large Diameter Pulsating Heat Pipe Experiment on board REXUS 22", *34th UIT Conference* 4-6 July 2016, Ferrara, Italy.
- [18] Nannipieri P., Anichini M., Barsocchi L, Becatti G., Buoni L., Celi F., Catarsi A., Di Giorgio P., Fattibene P. Ferrato E., Guardati P., Mancini E., Meoni G., Nesti F., Piacquadio S., Pratelli E., Quadrelli L., Viglione A. S., Zanaboni F., Mameli M., Baronti F., Fanucci L., Marcuccio S., Bartoli C., Di Marco P., Bianco N., Marengo M., Filippeschi S., 2017. "The U-PHOS

experience within the ESA studentREXUS/BEXUS programme: a real space hands-on opportunity”, IEEE EDUCON Conference 2017.

- [19] Nannipieri P., Meoni G., Nesti F., Mancini E., Celi F., Quadrelli F., Ferrato E. Guardati P., Fanucci L., Signorini A., Nannipieri T., 2017. “Application of FBG sensors to temperature measurement on board of the REXUS 22 sounding rocket in the framework of the U-PHOS project”, IEEE METrology for areospace international workshop 2017.
- [20] Mameli M., Mangini D., Vanoli G., Filippeschi S., Araneo L., Marengo M., 2016. “Advanced Multi-Evaporator Loop Thermo-syphon”, *Energy Int. J.*, 10.1016/j.energy.2016.06.074.
- [21] Di Giorgio P., Iasiello M., Viglione A. S., Mameli M., Filippeschi S., Di Marco P., Andreozzi A., Bianco N., 2017. “Numerical Analysis of a Paraffin/Metal Foam Composite for Thermal Storage”, *J. Phys.: Conf. Ser.* **796** 012032